Ji *et al. BMC Oral Health* (2025) 25:720
https://doi.org/10.1186/s12903-025-06068-1

BMC Oral Health

RESEARCH

Open Access

Evaluating the feasibility of conventional and digital impressions of full-arch by the absolute linear deviation method: an in vitro study

Jianhua Ji[1,3†], Luming Wei[2†], Xuzhe Zha[3], Huiying Guo[2] and Penglai Wang[2,3*]

Abstract

Background Intraoral scanners (IOS) facilitate dental treatment, but the efficacy in full-arch scanning remains controversial. The aim of this study was to compare arch deformations between conventional impressions (CIs) and digital impressions (DIs) across six distinct spans in the maxillary and mandibular models, using the absolute linear deviation method.

Methods Standard maxillary and mandibular models, each with seven cylindrical landmarks added, were used as the reference. CIs and DIs as test scans ($n = 15$ each) were performed on the models using silicone impression material and three IOSs: CS3600, Trios3, and Trios5. The trueness of the distances and angles between the remaining cylinders and initial scanning cylinder were evaluated. Data were analyzed using the Kruskal-Wallis and One-way ANOVA tests, with the Bonferroni test for post hoc analysis ($\alpha = 0.05$).

Results Deviations of DIs increased gradually from smaller spans to full-arch spans, while deviations of CIs remained stable. Within a 5-tooth-units, DIs provided superior trueness compared to CIs ($P < 0.05$), except for ΔL8, where the results from four impression methods were comparable ($P = 0.28$). For other measurements, CIs exhibited significantly better trueness than three IOSs ($P < 0.05$).

Conclusions The current accuracy of IOSs was insufficient for full-arch applications, but suitable for short scan ranges (fixed prostheses within a 5-unit span).

Keywords Intraoral scanners, Scanning spans, Absolute linear deviation method, Trueness

†Jianhua Ji and Luming Wei contributed equally to this article and should be regarded as co-first authors.

*Correspondence:
Penglai Wang
penglai_w0806@163.com
[1]Department of Implantology, Suzhou Stomatological Hospital, Suzhou, China
[2]Department of Oral Implantology, The Affiliated Stomatological Hospital of Xuzhou Medical University, 130 Huaihai West Road, Xuzhou 221003, PR China
[3]School of Stomatology, Xuzhou Medical University, 209 Tongshan Road, Xuzhou 221004, PR China

Background

With the rise of digital concepts in dentistry, intraoral digital impressions (DIs) have become increasingly prevalent. Compared to conventional impressions (CIs), DIs offer several advantages, including enhanced comfort, higher efficiency, and improved patient-doctor communication [1–3]. Additionally, the integration of chairside computer-aided design and computer-aided manufacturing (CAD/CAM) with IOSs can significantly accelerate the restorative treatment process [4, 5]. As a result, the use of IOSs to capture DIs will become a trend.

Chen et al. [6] reported the that scan spans affected the accuracy of the IOSs. It had been confirmed that single-crown and short-span scans were more accurate than CIs [7–10], and that half-arch scans were more accurate than full-arch scans [6, 11, 12]. It was largely due to the limited field of view (FOV) of the scanning head, which requires IOSs to use a best-fit algorithm to align and stitch the acquired sequential images to reconstruct the dental surface. During this process, stitching errors progressively accumulated as the span increased, leading to a decrease in accuracy toward the latter part of the scan [13, 14].

Recent studies have evaluated the accuracy of full-arch scans using various methods [10, 15–21], including the best-fit method and the absolute linear deviation method. The best-fit method involved a three-dimensional visualization of the test scan superimposed on the reference scan for comparison [22], utilizing a sampling volume of thousands of points. However, this approach could introduce errors due to the high sampling density, where pixels at non-identical locations could be incorrectly aligned, leading to an underestimation of accuracy [23]. In contrast, the absolute linear deviation method provided a precise quantitative assessment of the distances between specific points on the model surface, without relying on global fitting, thereby minimizing errors. Lyu et al. [24] compared the two methods in terms of accuracy assessment and found the absolute linear deviation method to be more sensitive.

Standard geometric objects are often used as references for evaluating the accuracy of full-arch scanning. Braian et al. [15] evaluated the accuracy of various IOSs by using five cylinders as landmarks across the full-arch. However, their anterior landmarks were detached from the dentition and did not accurately represent the true anterior deformations. Kuhr et al. [19] used prefabricated metal-assisted spheres fixed to the mandibular dentition and compared the accuracy between DIs and CIs. However, the four spheres were scattered, failing to capture the changes in accuracy across different spans of the impressions.

The present study extended previous research by adding seven cylindrical landmarks to both the maxillary and mandibular models. This addition facilitated more detailed segmentation and enabled precise measurements across six distinct spans. This study aimed to assess the differences in trueness between CIs and three IOSs across various spans. The null hypothesis was that all four impression techniques would demonstrate comparable trueness at any given span within the full-arch.

Methods

Design and fabrication of the master model

The standard tessellation language (STL) files of the standard maxillary and mandibular models were imported into the reverse engineering software (Studio 2014, Geomagic, Morrisville, NC, USA). Cylindrical landmarks were then placed at the positions of the second molar, second premolar, canine, and mesial incisors at the midline, with a diameter of 4 mm and a height of 3 mm above the dentition. The maxillary landmarks were labelled A-G from left to right, while the mandibular landmarks were labelled H-N from right to left. The experimental models were subsequently manufactured using a 3D printer (AccuFab-L4D, Xianlin 3D, Hangzhou, China) with 50 μm tolerance and AccuFab DM12 resin (Xianlin 3D, Hangzhou, China) (Fig. 1).

Scanning procedure

All scanners were calibrated according to the manufacturer's guidelines before scanning. The two models were then scanned using three IOSs (CS3600 (Carestream Dental, Rochester, USA) with software version 7.0.23.0.d2; Trios3 (3Shape, Copenhagen, Denmark) with software version 1.7.82.5; and Trios5 (3Shape, Copenhagen, Denmark) with software version 1.7.83.0.) (Table 1) following the recommended scanning strategies provided by the manufacturer. In the maxillary model, the scanning procedure encompassed the occlusal and incisal surfaces from the left to the right second molars, followed by the lingual and buccal surfaces. In the mandibular model, the scanning began at the right second molars and followed the same strategy of the maxilla. (Fig. 2). Each maxillary and mandibular model was scanned 15 times. The models were then digitalized using a dental laboratory scanner (CERAMILL MAP 600; Amann Girrbach, Germany) to obtain reference scans, which were exported in STL format. The digital models were checked for deficiencies, with re-scanning performed if necessary. All procedures were conducted under consistent scanning conditions (ambient light, temperature, and humidity).

Conventional impression

Disposable plastic trays of appropriate size were selected, and polyvinyl siloxane impressions (Silagum-Light/Silagum-MixStar Putty Soft; DMG Medical Devices) were taken using a two-step impression technique at room temperature. After setting for half an hour, the

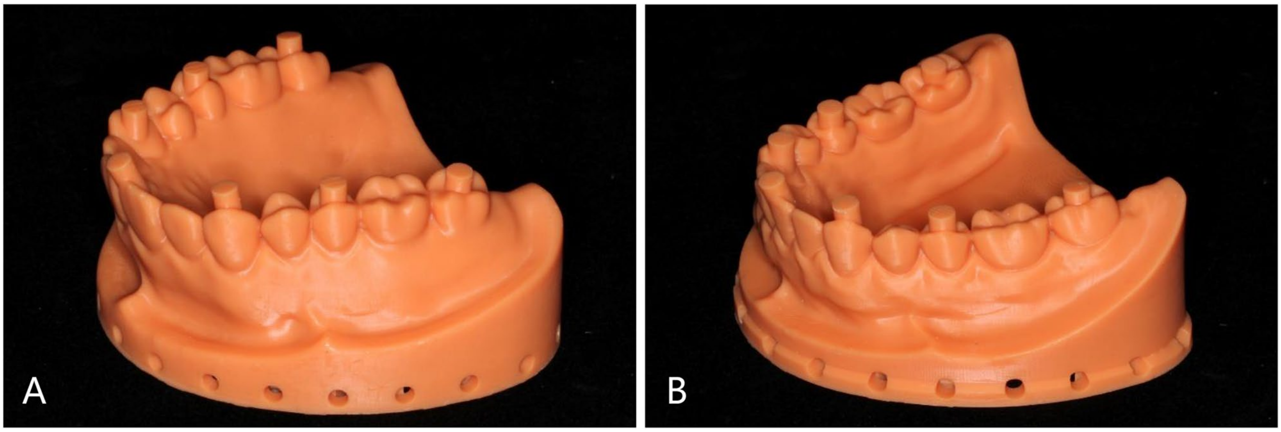

Fig. 1 The 3D printed resin experimental models with cylindrical landmarks. **A**. Maxillary experimental model. **B**. Mandibular experimental model

Table 1 The general information of IOSs used in this study

IOS	Producer	Technology of acquisition	Powder	Colour	Software Version
CS 3600 ®	Carestream Dental, Atlanta, Georgia, USA	Structured light-Active Speed 3D Video™	No	Yes	7.0.23.0.d2
Trios 3 ®	3-Shape, Copenhagen, Denmark	Structured light-Confocal microscopy and Ultrafast Optical Scanning™	No	Yes	1.7.82.5
Trios 5 ®	3-Shape, Copenhagen, Denmark	Structured light-Confocal microscopy and Ultrafast Optical Scanning™	No	Yes	1.7.83.0

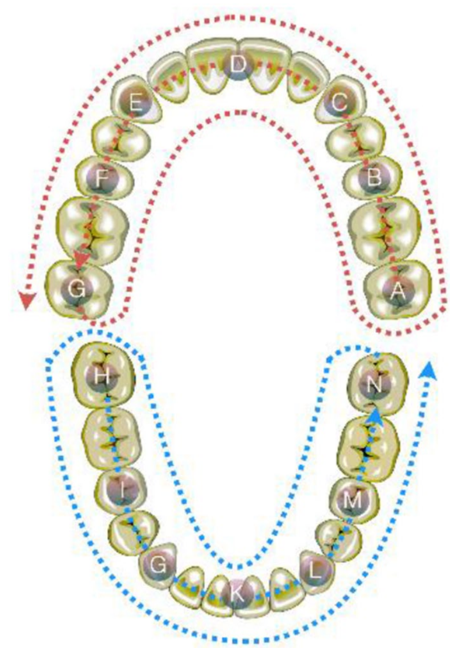

Fig. 2 Schematic diagram of the full-arch scanning strategy. The letters A-G/H-N indicate the position of landmarks in the maxillary and mandibular models respectively

impressions were poured with type IV gypsum. Following the complete setting of the stone, the maxillary and mandibular cast were scanned and digitized using a dental laboratory scanner. This procedure was repeated 15 times to generate STL files, which were then exported. All impressions were made by one dentist with extensive experience in full-arch conventional and digital impression making.

Processing of scan data

The STL files of the reference and test scans were imported into the Geomagic Studio 2014 software. The cylindrical structure in the scan data was selected using the Mark function, and cylindrical features were created based on the marked surface using the best-fit cylinder function (Fig. 3A). Next, the Convert function was utilized to convert the features into standard cylindrical objects, which were imported into forward engineering software (3-matic Research 11.0, Materialise, Belgium) to create the top surface centers and axes (Fig. 3B).

For the maxillary model, the leftmost landmark (A) was selected as the reference. The linear distances from the center of the top surface of each remaining landmark to the center of the reference landmark were calculated and labelled as L1–L6. Additionally, the angles between the axis of each landmark and the axis of the reference landmark were calculated and labelled as A1–A6. For the mandibular model, the rightmost landmark (H) was chosen as the reference. The same method was applied as the

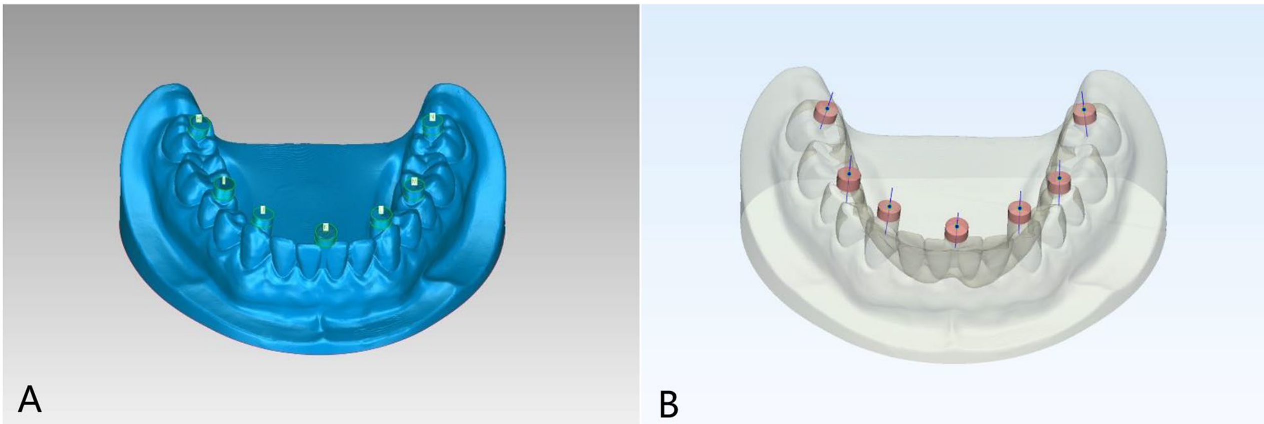

Fig. 3 Processing of scan data. **A**. Landmarks in STL data were fitted to standard cylinder geometry. **B**. Create top center and axis for each standard cylinder object. STL, standard tessellation language

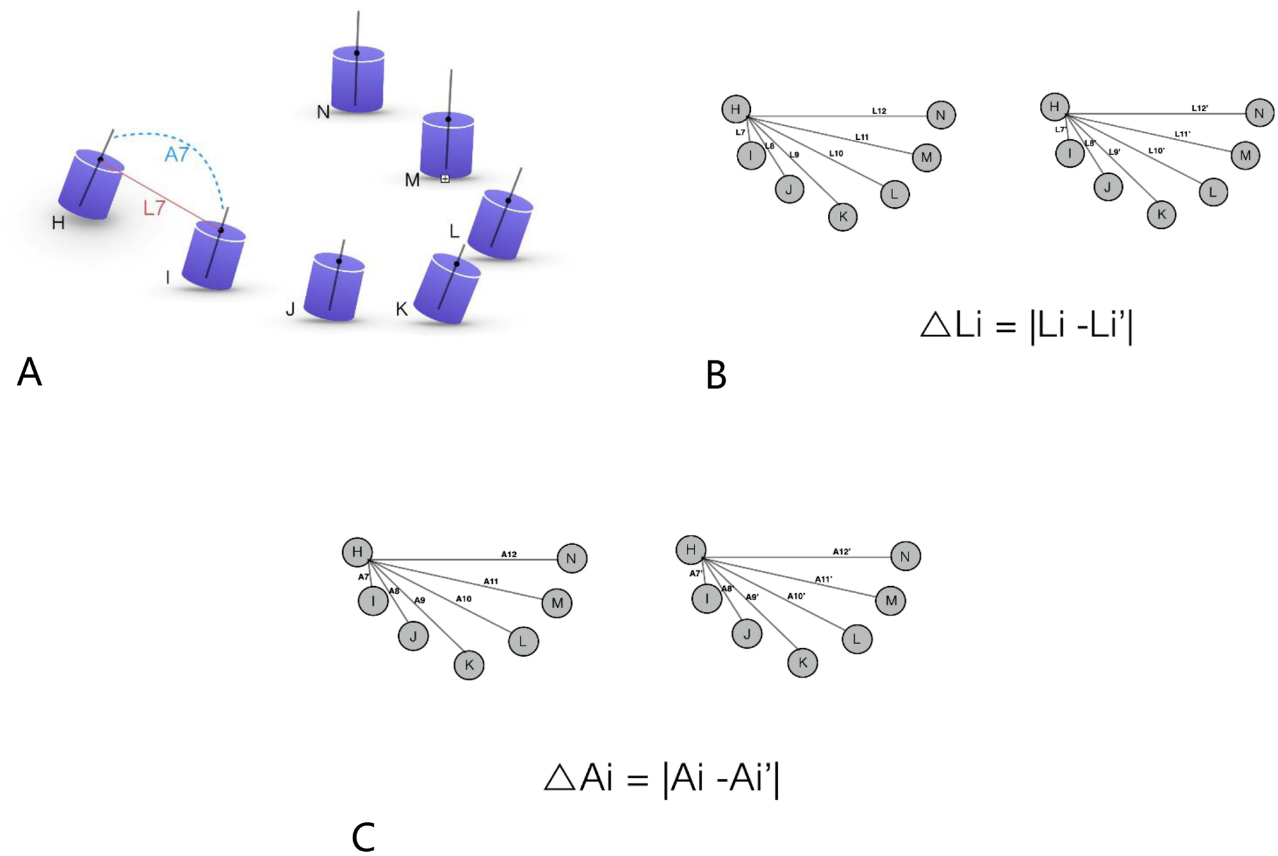

Fig. 4 Schematic diagram of the trueness evaluation, using the mandibular model as an example. **A**. Calculation of the point-to-point distances (Li) and line-to-line angles (Ai) between the remaining cylinders and the initial scanning cylinder. The linear and angular deviations between the I and H landmarks were recorded as L7 and A7. **B**. Value of linear deviations (ΔLi) between test (Li) and reference (Li') STL files. **C**. Value of angular deviations (ΔAi) between test (Ai) and reference (Ai') STL files

maxillary model, with the linear distances defined as L7–L12 and the angles defined as A7–A12.

According to ISO 5725-1, trueness refers to the closeness between the test data and the reference data. The linear difference (ΔLi =|Li-Li'|) and the angular difference (ΔAi =|Ai-Ai'|) between the test and reference STL files for each landmark were used to determine the trueness in this study (Fig. 4).

Statistical analysis

Based on the results of pre-experimentation, a sample size of $n = 15$ per group was sufficient to produce a Type

Table 2 The median and IQR of linear trueness (μm) for four impression techniques

Scan span	Group				*P* value
	CS3600	Trios3	Trios5	CI	
ΔL1	18.80[16.70–23.90][b]	11.70[9.20-16.58][b]	15.90[10.25–17.70][b]	36.80[24.82–45.37][a]	< 0.001*
ΔL2	28.20[25.75–34.50][b]	22.60[18.05–28.45][b]	25.90[17.35–33.20][b]	35.25[25.31–47.30][a]	0.016
ΔL3	57.85[51.20–63.00][b]	72.50[63.90-80.85][a]	68.00[59.50-80.05][a]	31.34[20.94–51.84][c]	< 0.001*
ΔL4	86.50[80.83–92.31][a]	94.80[71.65-108.15][a]	90.70[80.60-106.50][a]	33.90[21.88–49.40][b]	< 0.001*
ΔL5	125.65[119.60-129.30][a]	148.80[126.15–160.10][a]	137.90[132.20-152.65][a]	46.68[36.30-64.49][b]	< 0.001*
ΔL6	201.10[197.30-207.20][a]	215.20[176.55-230.65][a]	209.20[192.25-221.95][a]	58.54[43.94–78.67][b]	< 0.001*
ΔL7	19.85[14.63-25.00][b]	14.60[11.40–20.80][b]	15.30[11.75–21.10][b]	35.21[24.40-40.94][a]	< 0.001*
ΔL8	31.70[28.25–34.45][a]	23.40[19.25–28.20][a]	27.20[21.55–38.75][a]	34.12[21.34–42.29][a]	0.28
ΔL9	61.00[57.20-76.65][b]	90.30[82.30-97.45][a]	71.30[61.70-79.45][b]	31.16[20.83–37.40][c]	< 0.001*
ΔL10	96.10[90.25–106.10][b]	146.60[122.95–150.90][a]	130.10[112.35-150.15][a]	32.45[19.78–46.03][c]	< 0.001*
ΔL11	146.50[132.70-155.55][b]	177.10[165.15-212.55][a]	156.50[142.20-195.90][b]	43.21[31.40-56.71][c]	< 0.001*
ΔL12	217.30[212.20-225.05][b]	258.80[234.25–277.10][a]	223.10[207.05-247.75][b]	59.32[51.82–72.43][c]	< 0.001*

IQR interquartile range; * Indicates significant difference ($P < 0.01$)

Lowercase letters indicate significant differences between different scanners

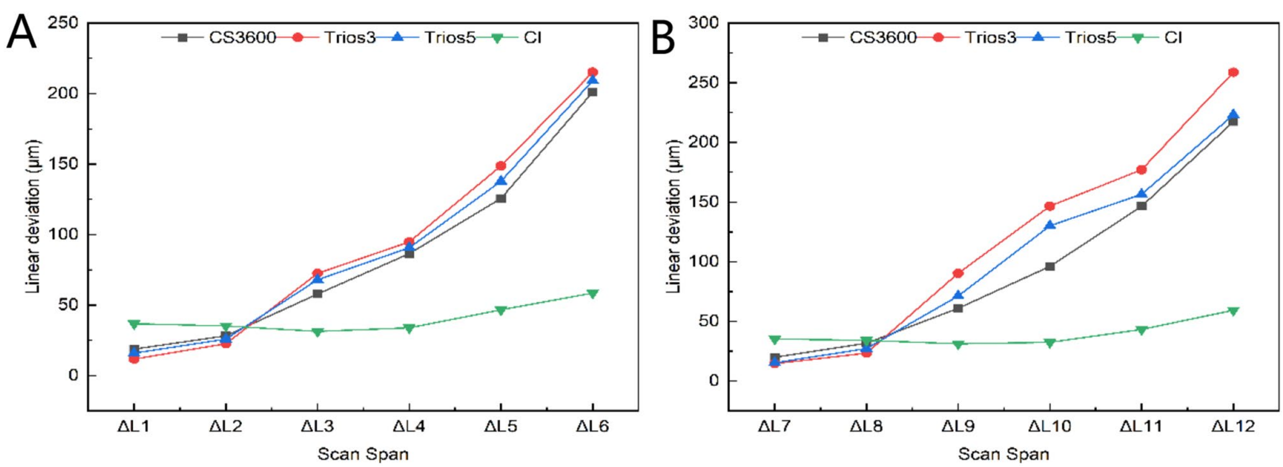

Fig. 5 Comparison of the linear deviations for each scanner according to the scan span. **A**. Linear deviations of the maxillary model at different spans. **B**. Linear deviations of the mandibular model at different spans

I error rate of 0.05 and power more than 80%. Statistical analysis was performed using SPSS 22.0 (IBM Corporation, Armonk, NY, USA). Descriptive statistics are shown as mean (SD) and median [IQR]. The Shapiro-Wilk test and Levene's test were used to assess the normality of the data and the homogeneity of variances, respectively. The results indicated that the linear deviation data followed a non-normal distribution, whereas the angular deviation data exhibited normality and homogeneity of variance. Therefore, the Kruskal-Wallis test was employed to analyze the differences in linear deviations (ΔL1-ΔL12), while one-way ANOVA was used to evaluate the differences in angular deviations (ΔA1-ΔA12). Post hoc analyses were performed using the Bonferroni test with a significance level set at $\alpha = 0.05$. This in vitro study did not require ethical approval.

Results

The results for the linear and angular deviations, based on an analysis of a total of 120 scans of maxillary and mandibular impressions taken by the four impression approaches, were presented in Tables and.

Figure 5 illustrates the linear deviations of four impression techniques across different spans of the maxillary and mandibular medels. For ΔL1, ΔL2, and ΔA7, no significant differences in trueness were observed among the three IOSs ($P > 0.05$), all of which outperformed CIs ($P < 0.05$). For ΔL8, no significant differences in trueness were found among four techniques ($P = 0.28$). For ΔL4-ΔL6, CIs showed superior trueness compared to the three IOSs ($P < 0.001$), with no significant differences among the IOSs themselves ($P > 0.05$). Regarding ΔL11 and ΔL12, CS3600 and Trios5 were comparable ($P > 0.05$), both superior to Trios3 ($P < 0.05$), but inferior to CIs ($P < 0.05$).

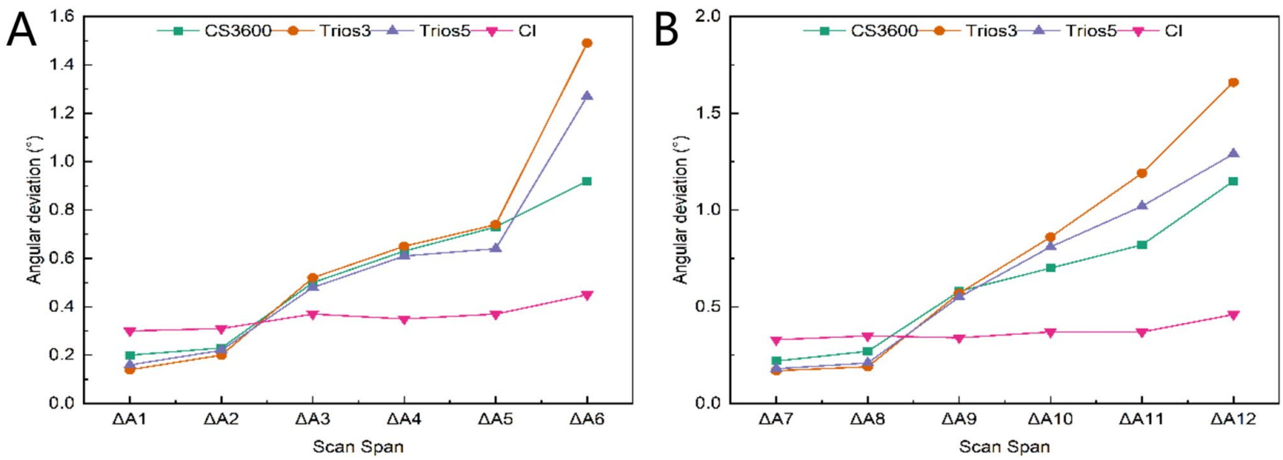

Fig. 6 Comparison of the angular deviations for each scanner according to the scan span. **A**. Angular deviations of the maxillary model at different spans. **B**. Angular deviations of the mandibular model at different spans

Table 3 The mean and SD of angular trueness (°) for four impression techniques

Scan span	Group CS3600	Trios3	Trios5	CI	*P* value
ΔA1	0.20 ± 0.07^{b}	0.14 ± 0.05^{b}	0.16 ± 0.07^{b}	0.30 ± 0.10^{a}	$< 0.001^{*}$
ΔA2	0.23 ± 0.10^{b}	0.20 ± 0.06^{b}	0.22 ± 0.09^{b}	0.31 ± 0.08^{a}	0.007^{*}
ΔA3	0.50 ± 0.12^{a}	0.52 ± 0.15^{a}	0.48 ± 0.12^{a}	0.37 ± 0.18^{b}	0.03
ΔA4	0.63 ± 0.16^{a}	0.65 ± 0.17^{a}	0.61 ± 0.12^{a}	0.35 ± 0.15^{b}	$< 0.001^{*}$
ΔA5	0.73 ± 0.10^{a}	0.74 ± 0.15^{a}	0.64 ± 0.16^{a}	0.37 ± 0.16^{b}	$< 0.001^{*}$
ΔA6	0.92 ± 0.15^{c}	1.49 ± 0.14^{a}	1.27 ± 0.20^{b}	0.45 ± 0.16^{d}	$< 0.001^{*}$
ΔA7	0.22 ± 0.07^{b}	0.17 ± 0.06^{b}	0.18 ± 0.09^{b}	0.33 ± 0.11^{a}	$< 0.001^{*}$
ΔA8	0.27 ± 0.08^{b}	0.19 ± 0.09^{b}	0.21 ± 0.07^{b}	0.35 ± 0.13^{a}	$< 0.001^{*}$
ΔA9	0.58 ± 0.11^{a}	0.57 ± 0.14^{a}	0.55 ± 0.14^{a}	0.34 ± 0.15^{b}	$< 0.001^{*}$
ΔA10	0.70 ± 0.09^{b}	0.86 ± 0.11^{a}	0.81 ± 0.16^{a}	0.37 ± 0.16^{c}	$< 0.001^{*}$
ΔA11	0.82 ± 0.1^{c}	1.19 ± 0.18^{a}	1.02 ± 0.16^{b}	0.37 ± 0.13^{d}	$< 0.001^{*}$
ΔA12	1.15 ± 0.08^{c}	1.66 ± 0.15^{a}	1.29 ± 0.16^{b}	0.46 ± 0.14^{d}	$< 0.001^{*}$

SD standard deviation; * Indicates significant difference ($P < 0.01$)

Lowercase letters indicate significant differences between different scanners

Figure 6 illustrates the angular deviations of the maxillary and mandibular models. For ΔA1, ΔA2, ΔA7, and ΔA8, the three IOSs significantly outperformed CIs ($P < 0.05$). Conversely, for ΔA3-ΔA6 and ΔA9-ΔA12, CIs demonstrated superior trueness compared to the IOSs ($P < 0.05$) (See Table 3).

Discussion

This study compared the differences in arch deformations among four impression techniques across six different spans in the maxilla and mandible by the absolute linear deviation method. The experimental results revealed significant differences in linear and angular deviations across all spans, except for ΔL8 in the mandible. Therefore, the null hypothesis was partially rejected.

Trueness was a critical reference value for fixed restorations [25]. It was recommended that scanning deviations of IOS should be limited to 100 μm [26, 27]. Exceeding the recommended threshold may result in biologic complications and mechanical complications, such as plaque retention, related periodontal problems and porcelain cracking [28, 29], which could compromise long-term treatment outcomes. In the present study, the linear deviations of DIs within a 3-unit scan range (measured as ΔL1 and ΔL7) were less than 20 μm, which was comparable to the results of a similar experiment [15], and the accuracy of the CIs was less accurate than DIs in the same range (ΔL1:36.80 μm; ΔL7:35.21 μm). It indicated that the IOS could achieve high scanning trueness within a 3-unit span. To our knowledge, no studies had measured linear deviations between second molar and canine, leaving a gap in the accuracy of 5-unit span comparisons. The present study found that CS3600, Trios3, and Trios5 exhibited significantly better ΔL2 trueness (28.20, 22.60, and 25.90 μm, respectively) than CIs (35.25 μm), while ΔL8 trueness (31.70, 23.40, and 27.20 μm, respectively) was comparable to that of CIs (34.12 μm). Furthermore, for angle deviations within a 5-unit span of the maxilla and mandible (ΔA1, ΔA2, ΔA7, ΔA8), the trueness of the three DIs was within 0.3°, while all CIs exceeded 0.3°($P < 0.05$).

Previous studies have demonstrated that the accuracy of IOSs decreased as the scanning span increased [6, 30]. Our findings were consistent with this trend. For the maxilla, when scanning beyond the midline to the contralateral canine (ΔL4), the trueness of the three IOSs remained below 100 μm, indicating an acceptable scanning range for restorative purposes of up to 9-units. In contrast, for the mandible, the trueness of ΔL10 for Trios 3 (146.60 μm) and Trios 5 (130.10 μm) both exceeded 100 μm, while the trueness ΔL10 for CS 3600 (96.10 μm) was also close to 100 μm. It could be attributed to the fact that the teeth in the mandibular anterior region, characterized by small, similar profiles and sharp edges, could degrade the image quality and propagate errors to subsequent scans [31]. Furthermore, this region is located on the turning point, which could further reduce the accuracy of image stitching during scanning [17, 32]. Based on the aforementioned results, the acceptable scanning range for restoration was limited to 7-units in the mandibular arch for both Trios 3 and Trios 5.

Further analysis revealed that the terminal deviations (ΔL6 and ΔL12) reached 200 μm for all IOSs, which were comparable to the results reported in a study of dentate human cadaver [21]. In the maxilla, CS 3600, Trios 3, and Trios 5 exhibited no significant differences in trueness of ΔL6. However, in the mandible, CS 3600 and Trios 5 showed comparable accuracy and outperformed Trios 3. Notably, CS 3600 exhibited the best linear and angular trueness in both maxillary and mandibular terminal scans, aligning with findings from several in vitro experiments [10, 18, 33]. Additionally, Trios 5 (software version 1.7.83.0) demonstrated superior performance compared to Trios 3 (software version 1.7.82.5) in both ΔL12 and ΔA12 trueness, which could be due to hardware and software upgrades [34–36]. Although scan span significantly affects the accuracy of IOS, several additional methods have been proven effective in improving full-arch scanning accuracy, such as using assistive devices during the scanning process, segmentation strategies, or a combination of IOS data with desktop scanning [37–39]. In both the maxilla and mandible, the linear trueness of CIs across six spans maintained within the range of 30–60 μm, all of which were within the acceptable deviation range. These findings aligned with those reported by Nagy et al. [21]. Meanwhile, the angular deviations ranged from 0.3°-0.5°, indicating that the spans had a limited effect on the CIs, with deviations almost uniformly distributed across the impression.

The primary limitation of this study was its in vitro nature. The absence of factors such as saliva, temperature changes, soft tissue displacement, and lighting variations [40–42], as well as the fact that all scans were performed by a single operator [43], could have a potential impact on the scanning process and accuracy. Additionally, since trueness is a critical reference value for fixed prosthodontic restorations [25], this study does not include precision assessment. However, it has been shown that reproducibility across multiple scans is also an important consideration in clinical practice, as the algorithms employed by IOSs may introduce variability between scans [44]. In this study, we incorporated cylindrical landmarks to facilitate measurements. However, this approach is not feasible in vivo conditions, and the added structures may have a potential influence on the scanning performance of the IOS [45]. The methodology selected for this study was based on the absolute linear deviation method. Although this approach offers certain advantages over Root Mean Square (RMS) calculations, such as avoiding the averaging of discrepancies, it is limited by its inability to capture three-dimensional deformations [46]. Given that deviations may involve six degrees of freedom, and the absolute linear deviation method primarily focuses on selected points rather than the overall scanning deformation, more scientifically robust evaluation methods, such as the novel approach proposed by Vág et al. [47] or the virtual fitting technique [27], should be considered for future investigations.

Conclusions

Within the limitations of the present in vitro study, the following conclusion could be drawn:

DIs are comparable or even superior to CIs within 5-units. Moreover, under clinically acceptable scanning deviations, the CS3600 is recommended for up to 9-units in both the maxilla and mandible, while the Trios3 and Trios5 are suitable for 9-unit maxillary and 7-unit mandibular impressions.

Abbreviations

Cis	Conventional impressions
DIs	Digital impressions
IOSs	Intraoral scanners
FOV	Field of view
STL	Standard tessellation language
3D	Three-dimensional
ANOVA	One-way analysis of variance
RMS	Root Mean Square

Acknowledgements

The authors thank all the participants and all the researchers who participated in this study. The authors also thank the Xuzhou Science and Technology Bureau for the funding support.

Author contributions

J.J. contributed to the conceptualization, methodology, validation, investigation, formal analysis, and writing - review & editing. L.W. contributed to the conceptualization, methodology, validation, investigation, formal analysis, and writing - Original Draft. X.Z. contributed to the methodology, validation, formal analysis, and writing - Original Draft preparation. H.G. contributed to the conceptualization, methodology, investigation, and resources. P.W. contributed to the conceptualization, methodology, data curation, writing - review & editing, supervision, project administration, funding acquisition. All authors have read and agreed to the published version of the manuscript.

Funding

This in vitro study was supported by the Science and Technology Bureau of Xuzhou city [grant numbers KC23150 & KC23221].

Data availability

The complete data and materials described in the research article are freely available from the corresponding author on reasonable request.

Declarations

Ethics approval and consent to participate

Not applicable.

Consent for publication

Not applicable.

Competing interests
The authors declare no competing interests.

Received: 19 December 2024 / Accepted: 28 April 2025
Published online: 14 May 2025

References

1. Cecilia G, Lorenzo F, Alessandro V, Marco F. Accuracy, reliability, and efficiency of intraoral scanners for full-arch impressions: a systematic review of the clinical evidence. Eur J Orthod. 2016;38:422–8.
2. Kihara H, Hatakeyama W, Komine F, et al. Accuracy and practicality of intraoral scanner in dentistry: A literature review. J Prosthodont Res. 2020;64:109–13.
3. Siqueira R, Galli M, Chen ZZ, et al. Intraoral scanning reduces procedure time and improves patient comfort in fixed prosthodontics and implant dentistry: a systematic review. Clin Oral Investig. 2021;25:6517–31.
4. Moussally C, Fron-Chabouis H, Charrière A, Maladry L, Dursun E. Full-mouth rehabilitation of Hypocalcified-type amelogenesis imperfecta with chairside Computer-aided design and Computer-aided manufacturing: A case report. Oper Dent. 2019;44:E145–58.
5. May J, Watson J. Restoration of a mandibular incisor with a Computer-aided Design/Computer-aided manufacturing fabricated anterior onlay. Oper Dent. 2019;44:109–13.
6. Chen YM, Zhai ZH, Watanabe S, Nakano T, Ishigaki S. Understanding the effect of scan spans on the accuracy of intraoral and desktop scanners. J Dent. 2022;124:104220.
7. Oh KC, Lee B, Park YB, Moon HS. Accuracy of three digitization methods for the dental arch with various tooth Preparation designs: an in vitro study. J Prosthodont. 2019;28:195–201.
8. Lee JJ, Jeong ID, Park JY, Jeon JH, Kim JH, Kim WC. Accuracy of single-abutment digital cast obtained using intraoral and cast scanners. J Prosthet Dent. 2017;117:253–9.
9. Nagata K, Fuchigami K, Okuhama Y, et al. Comparison of digital and silicone impressions for single-tooth implants and two- and three-unit implants for a free-end edentulous saddle. BMC Oral Health. 2021;21:464.
10. Park GH, Son K, Lee KB. Feasibility of using an intraoral scanner for a complete-arch digital scan. J Prosthet Dent. 2019;121:803–10.
11. Ahlholm P, Sipilä K, Vallittu P, Jakonen M, Kotiranta U. Digital versus conventional impressions in fixed prosthodontics: A review. J Prosthodont. 2018;27:35–41.
12. Revilla-León M, Gómez-Polo M, Barmak AB, Yilmaz B, Kois JC, Alonso Pérez-Barquero J. Influence of scan extension and starting quadrant on the accuracy of four intraoral scanners for fabricating tooth-supported crowns. J Prosthet Dent. 2024;18:S0022–3913.
13. Atieh MA, Ritter AV, Ko CC, Duqum I. Accuracy evaluation of intraoral optical impressions: A clinical study using a reference appliance. J Prosthet Dent. 2017;118:400–5.
14. Vitai V, Németh A, Solyom E, et al. Evaluation of the accuracy of intraoral scanners for complete-arch scanning: A systematic review and network meta-analysis. J Dent. 2023;137:104636.
15. Braian M, Wennerberg A. Trueness and precision of 5 intraoral scanners for scanning edentulous and dentate complete-arch mandibular casts: A comparative in vitro study. J Prosthet Dent. 2019;122:129–36.
16. Ciocan LT, Vasilescu VG, Rauta SA, Pantea M, Pituru SM, Imre M. Comparative analysis of four different intraoral scanners: an in vitro study. Diagnostics. 2024;14:1453.
17. Liu CT, Chen JH, Du JK, Hung CC, Lan TH. Accuracy comparison of scan segmental sequential ranges with two intraoral scanners for maxilla and mandible. J Dent Sci. 2024;19:466–72.
18. Son K, Jin MU, Lee KB. Feasibility of using an intraoral scanner for a complete arch digital scan, part 2: A comparison of scan strategies. J Prosthet Dent. 2023;129:341–9.
19. Kuhr F, Schmidt A, Rehmann P, Wöstmann B. A new method for assessing the accuracy of full arch impressions in patients. J Dent. 2016;55:68–74.
20. Van dMWJ, Andriessen FS, Daniel W, Yijin R. Application of Intra-Oral dental scanners in the digital workflow of implantology. PLoS ONE. 2012;7:e43312.
21. Nagy Z, Simon B, Mennito A, Evans Z, Vág J. Comparing the trueness of seven intraoral scanners and a physical impression on dentate human maxilla by a novel method. BMC Oral Health. 2020;20:97.
22. Revilla-León M, Gohil A, Barmak AB, Zandinejad A, Raigrodski AJ. Alonso Pérez-Barquero J. Best-Fit algorithm influences on virtual casts' alignment discrepancies. J Prosthodont. 2022;32:331–9.
23. Mangano F, Gandolfi A, Luongo G, Logozzo S. Intraoral scanners in dentistry: a review of the current literature. BMC Oral Health. 2017;17:149.
24. Lyu M, Di P, Lin Y, Jiang X. Accuracy of impressions for multiple implants: A comparative study of digital and conventional techniques. J Prosthet Dent. 2022;128:1017–23.
25. Ender A, Attin T, Mehl A. In vivo precision of conventional and digital methods of obtaining complete-arch dental impressions. J Prosthet Dent. 2016;115:313–20.
26. Chang MC, Cheng LW, Chuang SF, Chen YC. The influence of Pontic distribution on the marginal and internal gaps of CAD/CAM five-unit anterior zirconia framework. J Dent Sci. 2024;19:1105–15.
27. Borbola D, Mikolicz A, Romanszky L, et al. Complete-arch accuracy of seven intraoral scanners measured by the virtual-fit method. J Dent. 2024;149:105281.
28. Sailer I, Pjetursson BE, Zwahlen M, Haemmerle CHF. A systematic review of the survival and complication rates of all-ceramic and metal-ceramic reconstructions after an observation period of at least 3 years. Part II: fixed dental prostheses. Clin Oral Implants Res. 2007;18:86–96.
29. Kale E, Seker E, Yilmaz B, Ozcelik TB. Effect of cement space on the marginal fit of CAD-CAM-fabricated monolithic zirconia crowns. J Prosthet Dent. 2016;116:890–5.
30. Kernen F, Schlager S, Alvarez VS, Mehrhof J, Vach K, Kohal R, et al. Accuracy of intraoral scans: an in vivo study of different scanning devices. J Prosthet Dent. 2022;128:1303–9.
31. Richert R, Goujat A, Venet L, et al. Intraoral scanner technologies: A review to make a successful impression. J Healthc Eng. 2017;2017:8427595.
32. Radeke J, Vogel A, Schmidt F, et al. Trueness of full-arch IO scans estimated based on 3D translational and rotational deviations of single teeth-an in vitro study. Clin Oral Investig. 2022;26:3273–86.
33. Mangano FG, Hauschild U, Veronesi G, Imburgia M, Mangano C, Admakin O. Trueness and precision of 5 intraoral scanners in the impressions of single and multiple implants: a comparative in vitro study. BMC Oral Health. 2019;19:101.
34. Schmalzl J, Róth I, Borbély J, Hermann P, Vecsei B. The impact of software updates on accuracy of intraoral scanners. BMC Oral Health. 2023;23:219.
35. Schmidt A, Schlenz MA, Liu HY, Kämpe HS, Wöstmann B. The influence of Hard- and software improvement of intraoral scanners on the implant transfer accuracy from 2012 to 2021: an in vitro study. Appl Sci-Basel. 2021:11.
36. Vág J, Renne W, Revell G, Ludlow M, Mennito A, Teich ST, Gutmacher Z. The effect of software updates on the trueness and precision of intraoral scanners. Quintessence Int. 2021;52:636–44.
37. Wu HK, Wang J, Chen GH, Huang XQ, Deng FL, Li YM. Effect of novel prefabricated auxiliary devices attaching to scan bodies on the accuracy of intraoral scanning of complete-arch with multiple implants: an in-vitro study. J Dent. 2023;138:104702.
38. Iturrate M, Eguiraun H, Solaberrieta E. Accuracy of digital impressions for implant-supported complete-arch prosthesis, using an auxiliary geometry part-An in vitro study. Clin Oral Implants Res. 2019;30:1250–8.
39. Li JY, Chen ZZ, Wang HL. Calibrated intraoral scan protocol (CISP) for full-arch implant impressions: an in vitro comparison to conventional impression, intraoral scan, and intraoral scan with scan-aid. Clin Implant Dent Relat Res. 2024;26:879–88.
40. Camc H, Salmanpour F. Effect of saliva isolation and intraoral light levels on performance of intraoral scanners. Am J Orthod Dentofac Orthop. 2020;158:759–66.
41. Revilla-Leon M, Subramanian SG, Ozcan M, Krishnamurthy VR. Clinical study of the influence of ambient light scanning conditions on the accuracy (Trueness and Precision) of an intraoral scanner. J Prosthodont. 2020;29:107–13.
42. Revilla-Leon M, Gohil A, Barmak AB, et al. Influence of ambient temperature changes on intraoral scanning accuracy. J Prosthet Dent. 2023;130:755–60.
43. Revilla-Leon M, Kois DE, Kois JC. A guide for maximizing the accuracy of intraoral digital scans. Part 1: operator factors. J Esthet Restor Dent. 2023;35:230–40.
44. Lim JH, Park JM, Kim M, Heo SJ, Myung JY. Comparison of digital intraoral scanner reproducibility and image trueness considering repetitive experience. J Prosthet Dent. 2018;119:225–32.
45. Amornvit P, Rokaya D, Sanohkan S. Comparison of accuracy of current ten intraoral scanners. Biomed Res Int. 2021;2021:2673040.

46. Schmidt A, Benedickt CR, Schlenz MA, Rehmann P, Woestmann B. Accuracy of four different intraoral scanners according to different Preparation geometries. Int J Prosthodont. 2022;34:756–62.
47. Vag J, Nagy Z, Simon B, et al. A novel method for complex three-dimensional evaluation of intraoral scanner accuracy. Int J Comput Dent. 2019;22:239–49.

Publisher's note